J. Org. Chem. **1995,** *60,* 2841–2847

Theoretical and Experimental Evidence for Unsymmetrical Bridging in the Cation Derived from 2-*tert*-Cumyl-2-adamantanol and 2-Isopropenyl-2-phenyladamantane in Magic Acid Solution

Daniel T. Stoelting,[†] David A. Forsyth,[‡] and James L. Fry*[,†]

Department of Chemistry, The University of Toledo, Toledo, Ohio 43606-3390, and Department of Chemistry, Northeastern University, Boston, Massachusetts 02115

Received January 13, 1995[⊗]

A previously published 400 MHz ^{1}H and 101 MHz ^{13}C NMR study on the ionization (to **8**) of 2-*tert*-cumyl-2-adamantanol (**6**) and 2-isopropenyl-2-phenyladamantane (**7**) in cold (−20 to −78 °C) Magic Acid/SO_2ClF revealed spectroscopic features expected for a stable carbocation but did not allow for an unambiguous assignment of the exact structure for species **8**. To clarify this situation, the present paper reports the deuterium isotope effects on the ^{13}C NMR spectrum of **8** formed by ionization of a 1:2 mixture of 2-*tert*-cumyl-2-adamantanol and its dimethyl-d_6 isotopomer. The differences between the chemical shifts of the protiated and deuteriated ions were found to be the same at −60 and −40 °C. In the deuteriated compound, the C^+ center was shifted 1 ppm downfield, relative to the protium compound, whereas the quaternary ^{13}C atom was shifted 0.9 ppm upfield. This is strong evidence that **8** is a single phenyl-bridged ion and supports the assignment of the structure for **8** as a partially bridged 2-*tert*-cumyl-2-adamantyl cation. The experimental studies have been complemented with theoretical computations. We probed the potential energy surface (PES) of the $C_{19}H_{25}^+$ ion in the region of the 2-*tert*-cumyl-2-adamantyl cation using geometry optimizations at the semiempirical AM1 and ab initio HF/STO-3G, HF/3-21G, and HF/6-31G(d) levels of theory. At the highest level of Hartree–Fock (HF) theory used, the HF/6-31G* level, the C_s 2-*tert*-cumyl-2-adamantyl cation (**9**) which is stabilized by the interaction of the C^+ center with the phenyl p system is the predicted structure for **8**. Phenyl stabilization is indicated by the phenyl–C–C^+ bond angle of 92.63°. Correlation effects on the relative energies for the $C_{19}H_{25}^+$ ions were estimated through MP2/6-31G(d) single-point computations. The MP2 correlation-corrected energies again indicated that **8** is a partially bridged **9**; however, the minimum in the PES profile for phenyl bridging is shifted to 75°, a considerable increase in bridging and phenonium ion character. In contrast to the HF prediction and as seen in the previous paper with the $C_{12}H_{17}^+$ ion, MP2/6-31G* calculations predict that there is a minimum rather than a maximum along the phenyl-bridging coordinate. This minimum at 75° is about 10° larger than the minimum found for the $C_{12}H_{17}^+$ system and indicates the expected influence of the greater positive charge stabilization at the 2-adamantyl position versus the 2-propyl position. We have calibrated the theoretical method used by doing similar calculations on the $C_{12}H_{17}^+$ homologues that occupy the 2,3-dimethyl-3-phenyl-2-butyl cation section of the PES. Our theoretical study of this cation shows how the MP3- and the MP4(SDQ)/6-31G(d) levels would affect the predicted relative energies of the $C_{19}H_{25}^+$ ions and the structure of **8**. Use of the numbers obtained from the latter study gave estimated MP3/6-31G* and MP4(SDQ)/6-31G* PESs which still showed the partially bridged **9** to be the predicted structure for species **8** but with larger phenyl-bridging angles of 80 and 82°, respectively. We showed previously that solvent effects or theoretical error might cause the benzyl cation isomer to be stabilized by as much as 7 kcal/mol. However, even if the MP4(SDQ)/6-31G(d) energies are corrected so that the benzyl cation isomer of **9** is stabilized by an additional 7 kcal/mol, the partially phenyl-bridged 2-*tert*-cumyl-2-adamantyl cation is 3.3 kcal/mol more stable than it.

Introduction

A study of the ionization to **8** of 2-*tert*-cumyl-2-adamantanol (**6**) and 2-isopropenyl-2-phenyladamantane (**7**) at −78 °C in Magic Acid solution (SbF_5–FSO_3H/SO_2ClF, 1:4 by volume) was published previously.[1] In that work, the 400 MHz ^{1}H and 101 MHz ^{13}C NMR spectra were reported to be identical over the temperature range −20 to −78 °C and over a 48 h time span at −78 °C. The work concluded that, although the spectroscopic features might suggest a stable carbocation, the unusual values of the chemical shifts do not allow for an unambiguous assignment of the exact structure. The following part of this introduction will attempt to convey to the reader the nature of the problem first presented in ref 1.

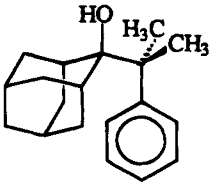

6

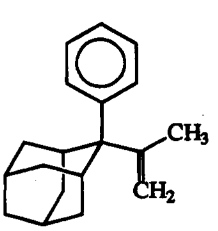

7

The chemical shift values for species **8** are shown in Figure 1 and are assigned to ^{13}C atoms of the most plausible single structure for **8**, the 2-*tert*-cumyl-2-

---

[†] The University of Toledo.

[‡] Northeastern University.

[⊗] Abstract published in *Advance ACS Abstracts*, April 15, 1995.

(1) Badejo, I. T.; Choi, H.; Hockensmith, C. M.; Karaman, R.; Pinkerton, A. A.; Fry, J. L. *J. Org. Chem.* **1991**, *56*, 4688–4696.

0022-3263/95/1960-2841$09.00/0

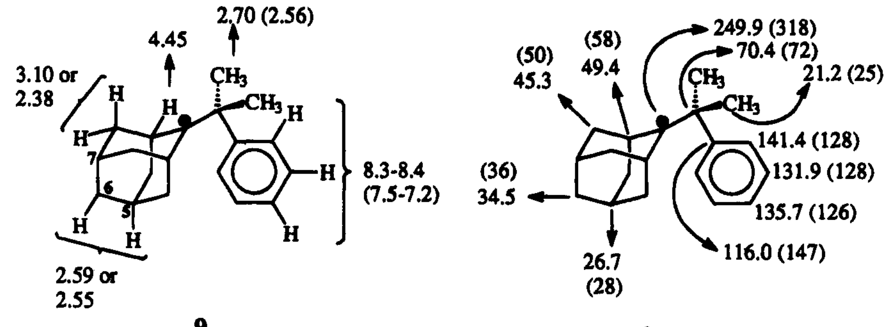

9 **9**

Figure 1. ^{1}H and ^{13}C NMR chemical shift assignments for **9** with reference to the 2-*tert*-cumyl-2-adamantyl cation structure.

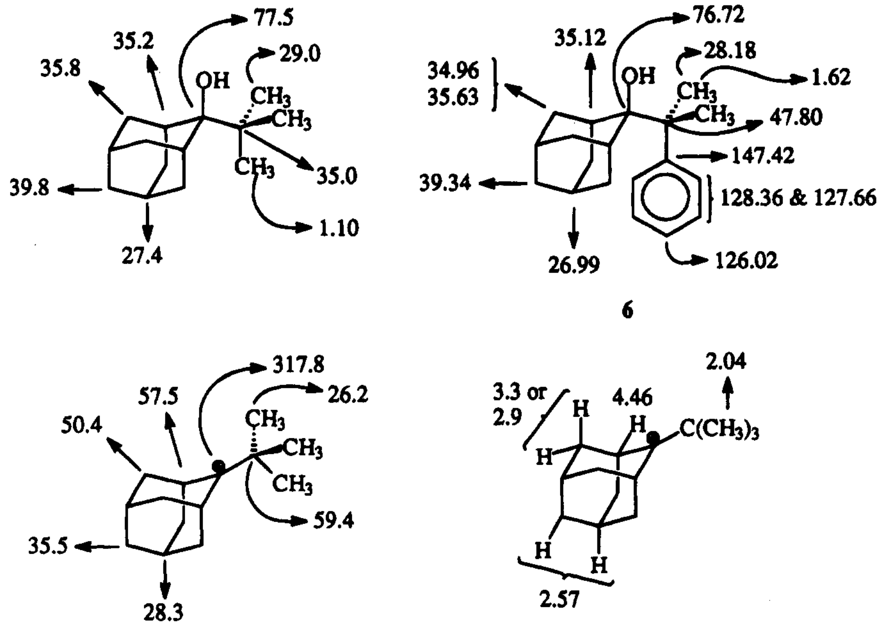

6

Figure 2. ^{13}C and ^{1}H chemical shift assignments for 2-*tert*-cumyl-2-adamantanol (**6**), 2-*tert*-butyl-2-adamantanol, and 2-*tert*-butyl-2-adamantyl carbenium ion.

adamantyl cation (**9**). Since the ^{1}H NMR chemical shifts reported in ref 1 for **8** were not internally referenced, we assumed that the protons attached to C5, C6, and C7 resonate at the same frequencies in the 2-*tert*-butyl-2-adamantyl cation[2] and **8** and corrected all other chemical shifts accordingly to give the values reported in Figure 1. That such an assumption is reasonable is demonstrated by the fact that the protons at the C5, C6, and C7 positions have almost identical chemical shifts for both 2-phenyl-2-adamantyl[3] and 2-*tert*-butyl-2-adamantyl cations. In parentheses are the values estimated for an unbridged **9** that has no interaction between the empty p orbital and a HOMO of the phenyl π system. A 101 MHz ^{13}C attached proton test (APT) NMR spectrum of **8** produced from **7** is consistent with the ^{13}C assignments in Figure 1.[4] The APT experiment differentiates the resonances of carbons attached to 0 and 2 protons from those of carbons attached to 1 and 3 protons.

The phenyl ^{13}C and ^{1}H resonances for unbridged **9** are the values found for the precursor alcohol **6**, while the adamantyl ^{13}C resonances for unbridged **9** are those found for the 2-*tert*-butyl-2-adamantyl cation. The ^{1}H and ^{13}C NMR resonances for the isopropyl group are those found for the 2-*tert*-butyl-2-adamantyl cation corrected by the substituent effects found from a comparison of the chemical shifts observed for 2-*tert*-butyl-2-adamantyl alcohol[2] with those of 2-*tert*-cumyl-2-adamantanol.[1] Proton and ^{13}C chemical shifts for the latter three species are presented in Figure 2.

Olah, Spear, and Forsyth faced a similar problem in the identification of **1** obtained in cold Magic Acid/SO$_2$ClF by ionizing the 2,3-dimethyl-3-phenyl-2-butyl chloride.[5] The results and conclusions of that study were reviewed in the previous paper.[6] It was found that **1** was mostly, if not completely, the α-*tert*-butyl-α-methylbenzyl cation (**2**) with little and probably no (tetramethylethylene)benzenium ion (**3**) or the 2,3-dimethyl-3-phenyl-2-butyl cation (**5**). This conclusion was strongly based on the ^{13}C chemical shifts exhibited by **1**. Our theoretical computations at the MP4(SDQ)/6-31G*//HF/6-31G* level showed that at −95 °C **2** is favored by only 0.29 kcal/mol over **3**, the next most stable isomer. At the same level, **5** was not an intermediate and the rotamer of **5**, **5-rot**, was the least favored ion by 4.64 kcal/mol relative to **2**. Since the MP4(SDQ) relative energies seemed sufficient

---

[2] Saba, J. A.; Fry, J. L. *J. Am. Chem. Soc.* **1983**, *105*, 533–537.

[3] Olah, G. A.; Liang, G.; Mateescu, G. D. *J. Org. Chem.* **1974**, *39*, 3750–3754.

[4] Badejo, I. T. Unpublished results.

[5] Olah, G. A.; Spear, R. J.; Forsyth, D. A. *J. Am. Chem. Soc.* **1977**, *99*, 2615.

[6] Stoelting, D. T.; Fry, J. L. *J. Org. Chem.* **1995**, *60*, xxx.

to predict the gas phase relative energies, the effect of solvation on the relative energies of the ions is believed to be the cause of the experimental observation of only **2**. Difference in the energy of solvation of the ions produces at the least a 2 kcal/mol stabilization of the benzyl cation **2** relative to **3** or **5**, but this value cannot be larger than 7 kcal/mol.

The dynamic processes that **8** can undergo in superacid at low temperatures are analogous to the ones discussed before for **1**.[6] For **8**, however, this situation is more complex since there are two semibridged β-phenyl cations possible: semibridged **9** and the other β-phenyl cation, semibridged **10**, which is analogous to semibridged **5**. Also, two different β-phenyl cations which are rotamers of **10** and **9**, **9-rot** and **10-rot**, are possible. These forms do not allow for positive charge stabilization by the phenyl group. We assume that consideration of the possibility of **9-rot**'s existence is sufficient, and we will not explicitly discuss **10-rot** from now on. Otherwise, the benzyl cation **11** is analogous to **2**, and the symmetrically or nearly symmetrically phenyl-bridged ion **12** is analogous to **3**.

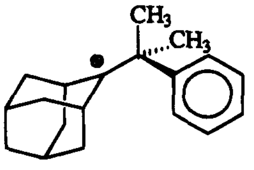

9-rot

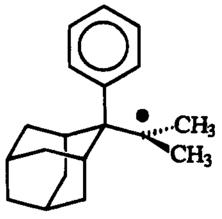

10

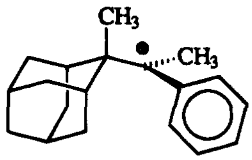

11

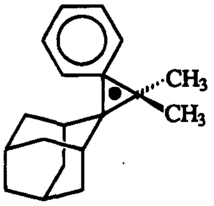

12

The additional cation, semibridged **9**, is unique because much positive charge is placed at the 2-carbon of the adamantyl ring system. Because the 2-*tert*-butyl-2-adamantyl cation is observed to be a stable species, as mentioned above, clearly phenyl-bridged **9** will be more stable than phenyl-bridged **10**. Species **12** is closely related to a semibridged **9** since it can be distinguished largely from how much bridging is occurring. Thus, we can probably eliminate semibridged **10** as a competitor and are left with the possibility that **11** and **9** or **12** make up the identity of **8**. We can expect that **9** and, to an extent, **12** will be more favored if not completely favored in the equilibrium with the benzyl cation **11**. This conclusion is based on the results in the previous paper for the analogous structures on the $C_{12}H_{17}^+$ PES and on the known greater stability that coincides with positive charge at a 2-adamantyl position rather than at a 2-propyl position.

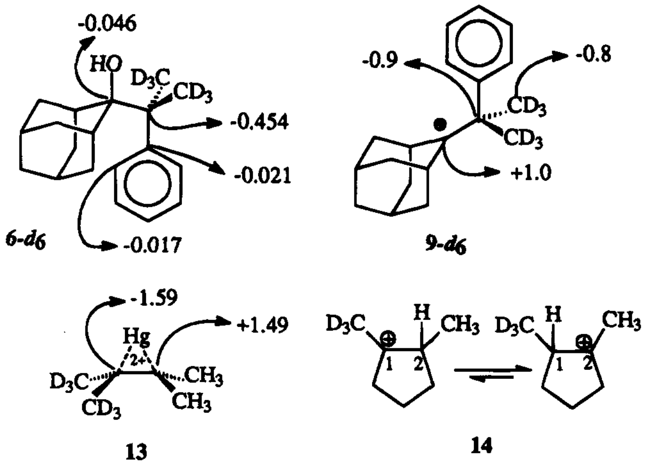

Figure 3. ^{13}C NMR isotope shifts in ppm. Shifts in the direction of shielding have a negative sign.

In agreement with the previous analysis, it is easiest to assign the ^{13}C chemical shifts, as was done in Figure 1, as resulting totally from a single species, a semiphenyl-bridged **9**. The quaternary carbon's resonance value of 70.4 ppm is particularly compelling since it is not much different from the estimated value of 72 ppm derived from the value found for the quaternary carbon of the 2-*tert*-butyl-2-adamantyl cation and the α-substituent effect (+12.8 ppm) on the ^{13}C chemical shift upon replacing a methyl group with a phenyl group implied in Figure 2. If any significant amounts of the benzyl cation or the other β-phenyl cation **10** were present, this resonance would be expected to be at a much lower field. Also, partial bridging is shown by comparing the classical cation values with the experimental values. In particular, all adamantyl carbons except C5, C6, and C7 show significant shielding, whereas all phenyl carbons and protons except the ipso carbon show significant deshielding. One particularly good indication of bridging is the chemical shift for the ipso carbon, which is ca. 20 ppm more shielded than the ipso carbon of a benzyl cation. For symmetrical bridging, one expects a value of ca. 101 ppm for the phenyl ipso or bridging carbon.[6]

Though the data are in favor of a single, unsymmetrically phenyl-bridged ion **9**, there are no precedents in the literature on which to firmly base such a conclusion. In addition, it is well-known that NMR chemical shifts are often average values of the various conformers present. In the present example, it is easy to suppose that the observed chemical shifts result from an equilibrium between **9-rot** and **12**, **9**, or some structure intermediate in the phenyl-bridging angle between **12** and **9**.

Results and Discussion

A. Isotopic Perturbation Study. The possibility that the unusual ^{13}C chemical shift in the 2-*tert*-cumyl-2-adamantyl cation is a consequence of a rapid equilibrium between two isomeric carbocations can be tested via isotopic substitution. In principle, any rapid equilibrium should be subject to an isotope effect in an appropriately labeled structure that would alter the position of the equilibrium, and the average positions of NMR signals, in a temperature-dependent fashion. Therefore, we have measured NMR isotope shifts in 75 MHz ^{13}C spectra of a 2:1 mixture of **9**-d_6 and **9**, prepared from a 2:1 mixture of the corresponding alcohols at −78 °C in 1:1 SbF_5–FSO_3H with CD_2Cl_2 and SO_2ClF as solvents. As shown in Figure 3, methyl deuteriation induces a one-bond NMR isotope shift, $^1\Delta C(D)$, of −0.8 ppm in the shielding direction at the methyl signal, a typical value for a deuteriated methyl group. A shielding $^2\Delta C(D)$ of −0.9

ppm is seen at the quaternary carbon, and a three-bond, deshielding isotope effect of ${}^3\Delta C(D) = +1.0$ ppm is seen for C^+ at −80 °C. Identical isotope shifts were measured at −60 and −40 °C. No isotope shifts were detected at any other carbons, but isotope shifts less than about 0.2 ppm would not be resolved due to the broad (~10 Hz) line widths of the carbocation solution. For comparison, ${}^{13}C$ NMR isotope shifts in the alcohol precursor determined at 20 °C in $CDCl_3$ are also shown.

The technique of isotopic perturbation has been particularly successful for distinguishing between a symmetrically bridged carbocation and a rapid degenerate equilibrium of classical carbocations.[7,8] A perturbed equilibrium between classical carbocations typically causes very large temperature-dependent NMR isotope shifts. Smaller intrinsic isotope shifts that show little, if any, temperature dependence are characteristic of symmetrically bridged species, such as σ-delocalized structures, and bromonium and mercurinium ions.[9] However, even in these bridged cations, the ${}^2\Delta C(D)$ and ${}^3\Delta C(D)$ intrinsic shifts are larger than they are in ordinary (uncharged) organic molecules where the ${}^2\Delta C(D)$ is typically less than −0.1 ppm per deuterium while ${}^3\Delta C(D)$ and longer range effects are even smaller in magnitude.[10] Perhaps the analogy closest to the current problem is the mercurinium ion, **13**-d_6, which gave the temperature-independent ${}^{13}C$ isotope shifts shown in Figure 3.[6] The C2 carbon bearing the deuteriated methyl groups moved in the direction of shielding, while C3 moved in the opposite direction, giving a C2−C3 shift difference of 3.1 ppm. In comparison, the chemical shift difference between C1 and C2 in the equilibrating ion, **14**, was much larger, 56.7 ppm at −81 °C and 43.4 ppm at −45 °C (shielded at C1, deshielded at C2).[7a]

The NMR isotope shifts in **9**-d_6 are of comparable magnitude to those seen in other bridged cations as well as unsymmetrically partially bridged species such as the 2-norbornyl cation[11] and show no temperature dependence. The lack of temperature dependence strongly indicates that the isotope shifts are intrinsic and that the 2-*tert*-cumyl-2-adamantyl cation exists as a single species. Although NMR isotope shifts are expected to be smaller for isotopic perturbation of a nondegenerate equilibrium where one species is substantially more populated than the other,[12] they should still be temperature-dependent. Furthermore, to explain a C^+ chemical shift of 250 ppm by equilibrating classic cations, a substantial fraction of a second classical ion would have to be averaged in with the principal ion, leading to the expectation that isotopic perturbation would still give quite large isotope shifts, although not as large as with the symmetrical ion, **14**.

Our search for the precise structure of **8** and theoretical support of the experimental findings through ab initio calculations is detailed in the next section.

B. Theoretical Search for 8. Our present experimental understanding of the structure of species **8** has been complemented with an understanding of the intrinsic relative stabilities of some key structures, which make up the 2-*tert*-cumyl-2-adamantyl cation region of the $C_{19}H_{25}{}^+$ potential energy surface (PES). Geometry optimizations at the AM1, HF/STO-3G, and HF/3-21G levels of molecular orbital (MO) theory were done. At the HF/6-31G(d) level, we optimized all bond, angle, and dihedral variables of **9** using C_s symmetry constraints with the phenyl group perpendicular to the plane of symmetry. Only the bond-and-angle variables of the other isomers were optimized at the HF6-31G(d) level. We enforced local C_s symmetry for the phenyl and adamantyl groups of **9-rot** and **11** and full C_s symmetry for **10**, **12**, and all other structures used to investigate the phenyl-bridging coordinate at all ab initio levels. While the latter symmetries were assumed for the AM1 calculations, the final geometries were usually performed without symmetry constraints. We attempted to gauge the influence of electron correlation through MP2/6-31G(d) single-point calculations on the HF/6-31G(d) geometries. As detailed in the previous paper, we also did a similar theoretical study of the $C_{12}H_{17}{}^+$ PES. In the latter study, it was feasible to do MP3- and MP4(SDQ)/6-31G(d) single-point computations. The latter ab initio study showed that the MP4(SDQ)/6-31G* result provides a reasonable picture of the PES for the types of ions we are studying. MP4(SDQ)/6-31G* single-point calculations on the $C_{19}H_{25}{}^+$ geometries are much too expensive so we employed the results of the $C_{12}H_{17}{}^+$ ab initio study to provide estimated values for points on the $C_{19}H_{25}{}^+$ MP3- and MP4(SDQ)/6-31G(d) PES.

1. Computational Details. Initial geometries were drawn with the interactive molecular-modeling program PCMODEL[13] and then minimized either by using PCMODEL or on the University of Toledo's VAX, MMX.[14] The AVS Chemistry Viewer on the University of Toledo's Kubota Pacific 3040 graphic supercomputer was useful in assigning **Z** matrices to some ions with the desired symmetry constraints. AM1 calculations[15] using MOPAC 5.0 and 6.0[16] and some ab initio calculations using Gaussian 90 were performed on the 3040 graphic supercomputer. The rest of the ab initio calculations, including all MP2/6-31G* single-point jobs, were done on the Ohio Supercomputer Center's CRAY Y-MP8/864 using either Gaussian 90 or Gaussian 92.[17] All MP2/6-31G* single-point calculations were performed using the frozen core approximation.

2. AM1 $C_{19}H_{25}{}^+$ PES. We began our theoretical study of the limited region of the $C_{19}H_{25}{}^+$ PES with the

---

[7] (a) Saunders, M.; Telkowski, L.; Kates, M. R. *J. Am. Chem. Soc.* **1977**, *99*, 8070. (b) Saunders, M.; Kates, M. R. *J. Am. Chem. Soc.* **1977**, *99*, 8071. (c) Saunders, M.; Kates, M. R.; Wiberg, K. B.; Pratt, W. *J. Am. Chem. Soc.* **1977**, *99*, 8072.

[8] Slehl, H. U. *Adv. Phys. Org. Chem.* **1987**, *23*, 63.

[9] Servis, K. L.; Domenick, R. L. *J. Am. Chem. Soc.* **1985**, *107*, 7186.

[10] For reviews of isotope shifts, see: (a) Hansen, P. E. *Annu. Rep. NMR Spectrosc.* **1983**, *15*, 106. (b) Forsyth, D. A. *Isot. Org. Chem.* **1984**, *6*, 1. (c) Jameson, C. J.; Osten, H. J. *Annu. Rep. NMR Spectrosc.* **1986**, *17*, 1. (d) Hansen, P. E. *Prog. NMR Spectrosc.* **1988**, *20*, 207. (e) Berger, S. *NMR* **1990**, *22*, 1.

[11] (a) Servis, K. L.; Shue, P. F. *J. Am. Chem. Soc.* **1980**, *102*, 7233. (b) Servis, K. L.; Domenick, R. L.; Forsyth, D. A.; Pan, Y. *J. Am. Chem. Soc.* **1987**, *109*, 1263. (c) Forsyth, D. A.; Botkin, J. H.; Puckace, J. S.; Servis, K. L.; Domenick, R. L. *J. Am. Chem. Soc.* **1987**, *109*, 7270.

[12] Forsyth, D. A.; Pan, Y. *Tetrahedron Lett.* **1985**, *41*, 4997.

[13] Gajewski, J. J.; Gilbert, K. E.; McKelvey, J. In *Advances in Molecular Modeling*; Liotta, D., Ed.; JAI Press: Greenwich, CT, 1990; Vol. 2.

[14] MMX 87.2 and 89.0 source code was kindly provided by J. J. Gajewski and K. E. Gilbert of Indiana University.

[15] Dewar, M. J. S.; Zoebisch, E. G.; Healy, E. F.; Steward, J. J. P. *J. Am. Chem. Soc.* **1985**, *107*, 3902.

[16] *MOPAC*, Version 6.00 and 5.0; Frank J. Seiler Research Laboratory: U.S. Air Force Academy, Colorado Springs, CO, 80840.

[17] (a) Frisch, M. J.; Head-Gordon, M.; Trucks, G. W.; Foresman, J. B.; Schlegel, H. B.; Raghavachari, K.; Robb, M.; Binkley, J. S.; Gonzalez, C.; Defrees, D. J.; Fox, D. J.; Whiteside, R. A.; Seeger, R.; Melius, C. F.; Baker, J.; Martin, R. L.; Kahn, L. R.; Stewart, J. J. P.; Topiol, S.; Pople, J. A. *Gaussian 90*, Revision H; Gaussian, Inc.: Pittsburgh, PA, 1990. (b) Frisch, M. J.; Trucks, G. W.; Head-Gordon, M.; Gill, P. M. W.; Wong, M. W.; Foresman, J. B.; Johnson, B. G.; Schlegel, H. B.; Robb, M. A.; Replogle, E. S.; Gomperts, R.; Andres, J. L.; Raghavachari, K.; Binkley, J. S.; Gonzalez, C.; Martin, R. L.; Fox, D. J.; Defrees, D. J.; Baker, J.; Stewart, J. J. P.; Pople, J. A. *Gaussian 92*, Revision B; Gaussian, Inc.: Pittsburgh, PA, 1992.

semiempirical AM1 method. There were only two processes to consider for **9**: (1) the 1,2-methyl shift and (2) the 1,2-phenyl migration. The transition states (TSs) of the latter two processes were located first by designating a variable as the reaction coordinate. For the latter purpose, the bond angle formed by the migrating carbon, the carbon to which it migrates, and the carbon bound to these two carbons, which is the corner of the angle, was used. Next, for each chosen value of the angle from one initial state (IS) **9** to the other, **10**, all other geometric variables were optimized with C_s symmetry enforced. Next, SADDLE calculations were done to obtain good first approximations of the TS structures for the phenyl migration process. For the methyl migration process, a structure from a reaction coordinate calculation, which is probably close in structure to the TS, was taken and used in the next step. The latter structures were then optimized using the TS keyword of MOPAC 6.0, which will try to ensure that the Hessian matrix has only one negative eigenvalue. For the methyl migration process, we found one TS, **9-rot-TS**, while for the phenyl migration process, we found two TSs, **9-TS** and **10-TS**.[18] The phenyl migration process has one more TS because of the existence of a phenonium structure **12** which is at a local minimum about midway along the phenyl-bridging coordinate that connects **9** with **10**.

The minimum energy reaction pathway (MERP) found as described above for process 2 was satisfactory since the TSs found fit right on the curve describing the section of the PES for phenyl migration. However, the MERP for the 1,2-methyl shift was more satisfactorily obtained by starting at the TS and proceeding to each ground state (GS). For the latter calculation, we first reminimized the TS with local C_s symmetry constraints for the phenyl and adamantyl groups before starting the calculation to reduce the number of variables. In addition, it was necessary to reminimize each structure found from the reaction coordinate study. The plots of the MERPs found for process 1 and 2 are given in Figure 4.

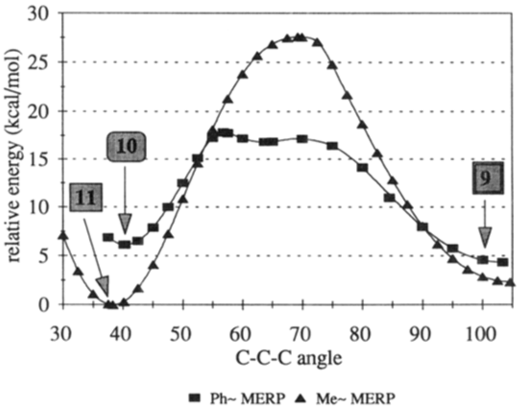

Figure 4. AM1 MERPs for the methyl and phenyl migration processes for the $C_{19}H_{25}^+$ ion in the 2-*tert*-cumyl-2-adamantyl cation region of the PES.

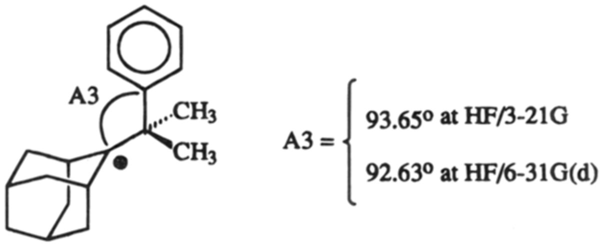

Figure 5. Predicted structure for **8** at the HF/3-21G and HF/6-31G(d) levels of theory.

Thus, the AM1 method erroneously predicts that the α-phenethyl cation **11** is more stable than **9-rot**, **9**, **10**, and **12** by 2.56, 4.33, 6.14, and 16.84 kcal/mol, respectively. Both **9** and **10** at the AM1 level have phenyl-bridging angles of 103.39 and 100.34°, respectively, which are less than the ideal tetrahedral value of ca. 109°. However, the rotamer of **9**, which cannot have phenyl stabilization, is predicted to be more stable than **9**. AM1 seriously underestimates the importance of β-phenyl stabilization of carbocations.

3. Hartree–Fock ab Initio PES. We went on to the ab initio restricted Hartree-Fock level of approximation using the geometries obtained at the AM1 level. Optimization of AM1 **9** using the HF/STO-3G basis set and enforced C_s symmetry produced a fully bridged cation (C_s STO-3G **12**). An HF/STO-3G frequency calculation yielded no imaginary vibrational frequencies. Except for **12**, we also partially optimized all AM1 ground state structures, **9-rot**, **10**, **9**, and **11**, at the HF/STO-3G level by optimizing the bonds and angles while freezing the AM1 dihedral angle variables. Such a strategy is expected to give reasonable energies for comparison with C_s STO-3G **12**. Thus C_s HF/STO-3G **12** is the predicted structure for **8** at this level of theory since it is more stable by 4.18, 4.30, 13.86, and 6.14 kcal/mol than **9-rot**, **9**, **10**, and **11**, respectively. Unlike the AM1 calculations, the HF/STO-3G calculations are moving toward agreement with experiment by showing that the α-phenethyl cation, **11**, is not the most stable, but they are still in disagreement because a nearly symmetrically phenyl-bridged structure is favored. As stated above, the experimental data are most consistent with a partially phenyl-bridged **9**.

When HF/STO-3G **12** was optimized at the HF/3-21G level with enforced C_s symmetry, a semibridged **9** was obtained. After **12** was optimized at the 3-21G level with the phenyl-C–C$^+$ bond held at the HF/STO-3G value of 65.44°, it is 8.83 kcal/mol less stable than **9**. Both experiment and the values for the $\phi-C_\beta-C_\alpha$ bond angle of 93.65° and the $\phi-C_\beta$ bond distance of 1.570 Å concur that there is a stabilizing interaction between a π molecular orbital of the phenyl group and the electron deficient p orbital. We optimized **9-rot** and **11** at the HF/3-21G level keeping local C_s symmetry for the phenyl and adamantyl groups. The 3-21G **9-rot** species is only ~1.3 kcal/mol less stable than HF/3-21G **9**. Species HF/3-21G **11** is 10.03 kcal/mol less stable than HF/3-21G **9**. Bond angles and bond distances, which would suggest no bridging, can be taken from the HF/3-21G structure for **9-rot**. These values are 16.34° larger and 0.032 Å smaller than the values found for C_s HF/3-21G **9**. On the other hand, the distortion from nearly symmetrical phenyl bridging is much larger than the distortion from the classical cation. The $\phi-C_\beta-C_\alpha$ angle is 28.21° larger and the $\phi-C_\beta$ bond distance 0.19 Å smaller for HF/3-21G **9** than the corresponding parameters for HF/3-21G **12**.

---

(18) An AM1 FORCE calculation proved that **10** had no imaginary frequencies. Species **10-TS** was optimized to a TS by means of MOPAC 6.0's TS keyword with the desired single imaginary frequency or "correct number of -VE roots". However, FORCE calculations revealed that **9** has two imaginary frequencies of 46.66i cm^{-1} and 6.40i cm^{-1}, **9-TS** has an extra imaginary frequency of 44.44i cm^{-1} in addition to the one for phenyl migration of 311.72i cm^{-1}, and **12** has one imaginary frequency of 36.33i cm^{-1}. Removal of symmetry constraints and reoptimization of **9-TS** and **12** in *XYZ* coordinates did not significantly change these findings. This situation is similar to what was found for the C_s 2,3-dimethyl-3-phenyl-2-butyl cation, **5**, in the previous paper[6] at the HF/3-21G and HF/6-31G(d) levels.

Table 1. Energies (kcal/mol) of $C_{19}H_{25}^+$ Ions Relative to the α-Phenethyl Cation 11

	level of theory						
species	AM1	HF/STO-3G	HF/3-21G	HF/6-31G*	MP2/6-31G*	estimated MP3/6-31G*	estimated MP4(SDQ)/6-31G*
9-rot	2.56	−1.96	−8.74	−5.77	−4.38	−4.59	−5.01
9	4.33	−1.83	−10.03	−7.99	−10.11	−7.97	−8.45
9(85)		10.97	−8.57	−6.94	−12.62	−9.89	−10.27
9(80)	14.12		−6.62	−5.61	−13.62	−10.17	−10.34
9(75)	16.44		−4.33	−4.12	−13.97	−10.00	−9.99
9(70)	17.18		−2.30	−2.84	−13.60	−9.39	−9.25
12	16.84	−6.14	−1.20	−2.06	−12.89	−8.63	−8.46
10	6.14	7.72	−2.58	−2.12	−7.92	−5.78	−5.57

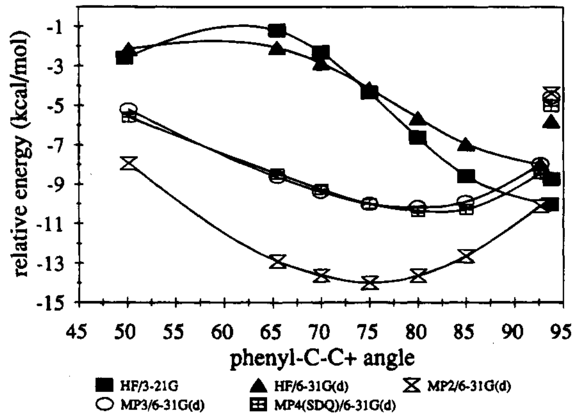

Figure 6. MERPs for phenyl migration in the $C_{19}H_{25}^+$ ion at the HF/3-21G, HF/6-31G(d), MP2/6-31G(d), and estimated MP3/6-31G(d) and MP4(SDQ)/6-31G(d) levels relative to the α-phenethyl cation. Additional symbols off of the interpolated lines and on the right side represent the relative energies for **9-rot**.

The alternative β-phenyl cation, **10**, was optimized within C_s symmetry at the HF/3-21G level and found to be disfavored relative to **9** by 7.45 kcal/mol. Thus, our theoretical structure for **8** is now consistent with experiment at the HF/3-21G level.

Next, we obtained structures representative of the phenyl migration section of the PES at the HF/3-21G level. These structures were used to investigate the nature of the surface at higher levels of theory as described below. AM1 structures obtained from the reaction coordinate calculation described above with bridging angles of 85, 80, 75, and 70° were used as the initial geometries. We did the full HF/3-21G optimization of each structure with enforced C_s symmetry and with the bridging angle fixed. The potential energy profile for phenyl migration shown in Figure 6 is well-behaved and so shows a satisfactory MERP has been found.

We next investigated the effect of polarization functions in the basis set by optimizing C_s HF/6-31G **9** at the HF/6-31G(d) level and found no significant change in geometry.[19] Compared with the HF/3-21G geometry, all bond variables changed by 0.01 Å or less; all angles changed by less than 1° except the bridging angle, which *decreased* by 1.03°, and all dihedral angle variables changed by less than 2°.

To measure the effect of adding polarization functions to the basis set on the relative energies of the other $C_{19}H_{25}^+$ ions, bond-and-angle HF/6-31G(d) optimizations were performed on the other HF/3-21G geometries. In summary, the $C_{19}H_{25}^+$ HF/6-31G(d) PES in the region of the 2-*tert*-cumyl-2-adamantyl cation is qualitatively the same as the HF/3-21G surface (also see Figure 6 and Table 1). Species **11** and **9** are still the least and most stable structures, respectively. Compared with the α-phenethyl cation **11**, the changes in energy going from the HF/3-21G to the HF/6-31G(d) level are +2.97, +2.04, +1.63, +1.01, +0.21, −0.54, −0.86, and +0.46 for **9-rot**, **9**, **9(85)**, **9(80)**, **9(75)**, **9(70)**, **12**, and **10**, respectively. Thus, as phenyl bridging decreases, the changes in energy get more positive so that the classical cation **9-rot** becomes less favored compared to the latter five isomers. Species **12**, it is noted, possesses the most bridging and is the only isomer to become more stable compared with **11**. These trends are the same ones observed for the simpler $C_{12}H_{17}^+$ system in the previous paper.[6]

4. MP2/6-31G(d) PES. Because MP2/6-31G(d) optimizations are too expensive to do on a structure the size of $C_{19}H_{25}^+$, we settled for single-point MP2/6-31G(d) computations to obtain correlation-corrected relative energies for the HF/6-31G(d)-optimized structures. The trend of classical **9-rot** becoming less stable compared to **11** continued since the energy difference was reduced by 1.39 kcal/mol. Species **9-rot** is then 4.38 kcal/mol more stable than **11**. The trend, noted at the HF level after introducing polarization functions into the basis set, where bridging is favored such that **12** and **9(70)** become more stable but all other isomers become less stable compared with **11**, is dramatically continued. Thus, **9**, **9(85)**, **9(80)**, **9(75)**, **9(70)**, **12**, and **10** are all *stabilized* by 2.12, 5.68, 8.01, 9.85, 10.76, 10.83, and 5.8 kcal/mol, respectively. The net result is that the most stable isomer is now the one with a phenyl-bridging angle of 75°. This extent of bridging seems to be more than one might expect in a linear approximation since the C^+ chemical shift of 250 ppm is only 68 ppm upfield from the estimated value for a classical 2-*tert*-cumyl-2-adamantyl cation but 161 ppm downfield from the estimated value for a symmetrically phenyl-bridged cation given in ref 6. This can be explained if the plot of the ^{13}C chemical shift versus the phenyl-bridging angle rises steeply as the angle increases from ca. 65° but then levels off. Just such a curve has been calculated for the 2-methyl-2-butyl cation using the IGLO method where the bridging carbon is part of a methyl group.[20]

The changes in relative energy found for the $C_{12}H_{17}^+$ ions between the MP3 and MP2 levels[6] were used to estimate MP3/6-31G(d) energies for the $C_{19}H_{25}^+$ ions. The

---

[19] The 6-31G geometry was obtained from the 3-21G geometry. Improvement in the description of the core molecular orbitals usually does not affect the geometry greatly. Such was the case for optimization of 3-21G **9** where only minor changes occurred. The most notable change was for the bridging variable, *A3*, which increased by 1.38°. Also, a frequency calculation indicated one small imaginary frequency equal to 23.78*i* cm^{-1}. Again, this is similar to what was found at the AM1 level[18] and in the previous paper[6] at the HF/3-21G and HF/6-31G(d) levels for **5**.

[20] Schleyer, P. v. R.; Carneiro, J. W. de M.; Forsyth, D. A.; Koch, W. *J. Am. Chem. Soc.* **1991**, *113*, 3990−3992.

MP3 estimates for the $C_{19}H_{25}^+$ isomers are given in the next to the last column of Table 1 and are also shown in Figure 5. Thus, we find that the semibridged **9** is still the favored species and that the benzyl cations **11**, **9-rot**, and **10** are still predicted to be too high in energy to be observed experimentally. Also, a little less bridging is predicted to occur since the minimum lies around **9(80)** for which the phenyl−C−C$^+$ angle equals 80°. The changes in relative energy found for the $C_{12}H_{17}^+$ ions between the MP4(SDQ) and MP2 levels were used to estimate MP4(SDQ)/6-31G(d) energies for the $C_{19}H_{25}^+$ ions. The MP4(SDQ) estimates for the $C_{19}H_{25}^+$ isomers are given in the last column of Table 1 and are also shown in Figure 6. A further shift in the minimum in the phenyl-bridging coordinate to 82° is predicted to occur at the MP4(SDQ) level.

Summary and Conclusions

Both the experimental and theoretical studies show that **8** is a single, unsymmetrically phenyl-bridged carbocation, **9**. Experiment did this through the technique of isotopic perturbation. Theory did this through high-level ab initio quantum chemical calculations, which revealed the nature of the PES for the $C_{19}H_{25}^+$ ion in the region of the 2-*tert*-cumyl-2-adamantyl cation.

Formation of the dimethyl-d_6 and -d_0 isotopomers of **8** in the same NMR tube allowed for the observation of the isotope effects on the ^{13}C spectra. The isotope effects on the ^{13}C resonances provided strong evidence as to whether **8** consists of intermediate ions in equilibrium or a single intermediate ion. Deshielding by 1.0 ppm at the C$^+$ center and shielding by 0.9 ppm at the quaternary carbon center were observed. Moreover, these effects were identical at −60 and −40 °C, i.e., these effects show temperature invariance. The size and direction of these effects fall in the category of large intrinsic isotope effects that are typically observed in single, static carbocations. Since these effects can be expected to vary significantly over the temperature range observed if an equilibrium of carbocations is involved, the insensitivity of these effects to temperature change implies that **8** is a partially phenyl-bridged carbocation. The introduction showed that the ^{13}C and ^1H NMR data are consistent with just such a structure, which is the partially phenyl-bridged 2-*tert*-cumyl-2-adamantyl cation.

Relative energies of the $C_{19}H_{25}^+$ ions in the region of the 2-*tert*-cumyl-2-adamantyl cation were found by MP2-(SDQ)/6-31G* single-point calculations on the C_s HF/6-31G* structure for **9** and on the HF/6-31G*(bonds & angles) structures for **9(85)**, **9(80)**, **9(75)**, **9(70)**, **9-rot**, **10**, **11**, and **12**. It was shown in the previous paper that this level of computation is not sufficient but that MP4-(SDQ)/6-31G* single-point calculations do provide a reasonable description of the $C_{12}H_{17}^+$ PES in the 2,3-dimethyl-3-phenyl-2-butyl cation region and that solvation effects or theoretical error might cause the calculated stability of the benzyl cation compared with the phenyl-bridged ions to be too high by at least 2 kcal/mol but by no more than 7 kcal/mol. The energy differences between the MP3/6-31G* and MP2/6-31G* levels and the MP4-(SDQ)/6-31G* and MP2/6-31G* levels reported in the previous paper were used to obtain estimated MP3 and MP4(SDQ) PESs for the $C_{19}H_{25}^+$ ions. In agreement with the isotopic perturbation study, the most stable isomer is shown to be a partially phenyl-bridged 2-*tert*-cumyl-2-adamantyl cation. This was favored by −10.4 kcal/mol over the benzyl cation **11** and had a phenyl-bridging angle of 82°. Even if solvation effects or theoretical error increased this energy by as much as 7 kcal/mol, as suggested above, the benzyl cation would still be disfavored by ca. 3.3 kcal/mol. Thus, theory appears to provide excellent proof that **8** is a single, partially phenyl-bridged 2-*tert*-cumyl-2-adamantyl cation.

Experimental Section

Preparation of Cation 8 and Observation by ^{13}C NMR Spectroscopy. Solutions of the ions were prepared, and determination of the spectra was performed as previously reported.[11b,c]

Preparation of 2-*tert*-Cumyl-2-adamantanol and Its Dimethyl-d_6 Isotopomer. These two alcohols were prepared in a manner similar to that reported in ref 1. The *tert*-cumyl-d_6 chloride used in the latter reaction to make the deuteriated isotopomer was prepared by a standard Grignard reaction of phenylmagnesium chloride with acetone-d_6.

Acknowledgment. We thank J. E. Gano for helpful comments and D. A. Smith for allowing us to use the AVS Chemistry Viewer program obtained through a grant from Molecular Simulations, Inc., and the Gaussian 90 and MOPAC 5.0 and 6.0 programs, obtained through a grant from The University of Toledo. We are grateful to the Ohio Supercomputer Center for a generous grant of time on the CRAY Y-MP8/864 computer. D.A.F. acknowledges the donors of the Petroleum Research Fund, administered by the American Chemical Society, for partial support of this work.

JO950102L